PHYSICAL REVIEW B **96**, 121406(R) (2017)

Nonlinear Dirac cones

Raditya Weda Bomantara,[1] Wenlei Zhao,[1,2] Longwen Zhou,[1,*] and Jiangbin Gong[1,†]
[1]*Department of Physics, National University of Singapore, Singapore 117543, Singapore*
[2]*School of Science, Jiangxi University of Science and Technology, Ganzhou 341000, China*
(Received 24 March 2017; published 27 September 2017)

Physics arising from two-dimensional (2D) Dirac cones has been a topic of great theoretical and experimental interest to studies of gapless topological phases and to simulations of relativistic systems. Such 2D Dirac cones are often characterized by a π Berry phase and are destroyed by a perturbative mass term. By considering mean-field nonlinearity in a minimal two-band Chern insulator model, we obtain a different type of Dirac cone that is robust to local perturbations without symmetry restrictions. Due to a different pseudospin texture, the Berry phase of the Dirac cone is no longer quantized in π, and can be continuously tuned as an order parameter. Furthermore, in an Aharonov-Bohm (AB) interference setup to detect such Dirac cones, the adiabatic AB phase is found to be π both theoretically and computationally, offering an observable topological invariant and a fascinating example where the Berry phase and AB phase are fundamentally different. We hence discover a nonlinearity-induced quantum phase transition from a known topological insulating phase to an unusual gapless topological phase.

DOI: 10.1103/PhysRevB.96.121406

Introduction. Starting with the seminal papers of Thouless *et al.* [1,2], the role of topology in the band theory of solids has attracted tremendous interest. In addition to topological insulators [3–5], the search for novel topological materials has led to the discoveries of Dirac [6–11], Weyl [12–15], and nodal-line semimetals [13,16–20]. Recently, topological phases in interacting systems have stimulated much attention [21–27]. After the topological classification of noninteracting topological insulators [28,29], a general topological classification of interacting systems constitutes an important topic [21,24,27].

Developing physical insights into the interplay of topology and interaction, which typically requires the use of advanced many-body techniques [30], is often a challenge. Simple mean-field approaches may be still useful [31–36]. Here, we take a modest mean-field approach to a minimal two-band topological insulator model with on-site bosonic interactions. This leads to a nonlinear problem, insofar as the Bloch states are now eigenstates of the Gross-Pitaevskii (GP) equation [37,38] depicting a two-dimensional (2D) tight-binding lattice with an on-site mean-field potential. GP equations are a well-known tool to study the Bose-Einstein condensate (BEC) of cold atomic gases, such as matter-wave solitons [39–41]. Moreover, GP equations are also useful in the study of photonic systems, where Kerr nonlinearity becomes important with the increase of light intensity [33,42,43]. We expect our theoretical predictions below to be relevant to simulations of topological quantum matter in cold-atom and photonic systems [44–46].

As already learned from zero- or one-dimensional systems, the band structure arising from solving the stationary GP equation may accommodate self-crossing loop (swallowtail) formations [47]. This feature in 2D situations suggests the loss of a well-defined band Chern number as a topological invariant. In the vicinity of the self-crossing point of a 2D looped band, we discover the formation of a different type of 2D Dirac cone. Such nonlinear Dirac cones (NDCs) share analogous robustness with Weyl points in Weyl semimetals [12–15].

Equally interesting, due to a peculiar pseudospin texture different from what is found in those familiar Dirac cones in 2D Dirac semimetals [6–11], NDCs yield Berry phases no longer quantized in π. Further, their band structure may be potentially useful for the quantum simulation of some exotic physics.

Following the stimulating experiment reported in Ref. [48], we propose to detect the formation of an NDC by use of an interference setup in the spirit of the Aharonov-Bohm (AB) effect [49].

As a remarkable finding detailed below, the AB phase associated with two adiabatic paths in the reciprocal space enclosing an NDC is still quantized in π. This provides a stimulating example where the Berry phase and AB phase are different. We shall also use this result to identify an experimentally accessible topological invariant for NDCs.

Two-band model. Consider a nonlinear version of the spinless (bosonic) two-band Dirac-Chern insulator model [50], with two sublattices serving as the pseudospin. With the lattice Hamiltonian detailed in Supplemental Material [51], the stationary GP equation in the momentum space assumes the following form,

$$\mathcal{H}[k_x,k_y,\psi(k_x,k_y)]|\psi(k_x,k_y)\rangle = E(k_x,k_y)|\psi(k_x,k_y)\rangle, \quad (1)$$

with

$$\mathcal{H}[k_x,k_y,\psi(k_x,k_y)] = J_x \sin(k_x)\sigma_x + J_y \sin(k_y)\sigma_y + \mathcal{B}(k_x,k_y)\sigma_z + g\begin{bmatrix} |\psi_1(k_x,k_y)|^2 & 0 \\ 0 & |\psi_2(k_x,k_y)|^2 \end{bmatrix}, \quad (2)$$

where σ's are Pauli matrices in the usual representation, k_x (k_y) is the quasimomentum along the x (y) direction, $|\psi(k_x,k_y)\rangle \equiv [\psi_1(k_x,k_y),\psi_2(k_x,k_y)]^T$ denotes a Bloch band state with two pseudospinor components, g is the nonlinear strength, $\mathcal{B}(k_x,k_y) = B[M + \cos(k_x) + \cos(k_y)]$, B is a parameter that may be interpreted as the hopping strength, M is related to the difference in potential strength between the two lattice species, and J_x and J_y mimic the effect

*zhoulw13@u.nus.edu
†phygj@nus.edu.sg

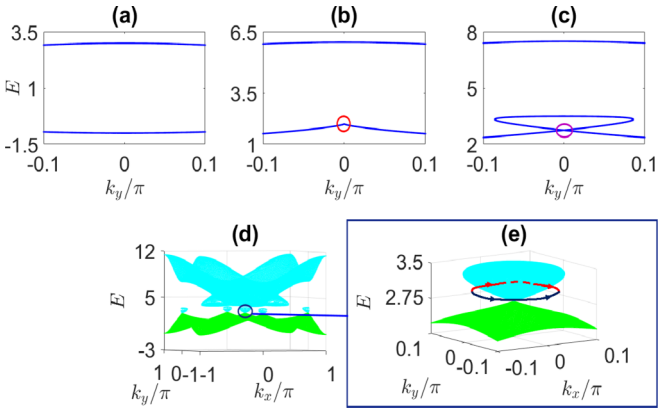

FIG. 1. The development of loop structure in the nonlinear Dirac-Chern insulator model. The parameters chosen are $M = -1$, $B = 2$, $J_x = J_y = 1$, $k_x = 0$, (a) $g = 1$, (b) $g = 4$, and (c) $g = 5.5$. The full spectrum over the 2D Brillouin zone is plotted in (d). (e) shows an enlarged version of (d) near a looped band structure. The red and blue curves in (e) illustrate two different interfering paths in a proposed AB-effect experiment.

of Rashba-like spin-orbit couplings. Throughout this Rapid Communication, all physical variables are assumed to be scaled and hence in dimensionless units. The linear version of the model here shares the same topological property with the Haldane model already realized in cold-atom systems [44], with its spinful counterpart [52] describing a quantum spin Hall insulator also realized experimentally [53]. Therefore, $\mathcal{H}[k_x,k_y,\psi(k_x,k_y)]$ is a representative and natural choice to accommodate bosonic mean-field interactions and to motivate experimental investigations.

Figures 1(a)–1(c) show the snapshots of the band structure near $k_y = 0$ at a fixed $k_x = 0$. As expected from previous theoretical and experimental studies of nonlinear Bloch bands in zero- or one-dimensional systems [47,54–61], a self-crossing loop structure emerges as g increases beyond a critical value g_c. Specifically, for $g = g_c$, the bottom band starts to develop a cusp [see the red circle in Fig. 1(b)]. For $g > g_c$, this cusp transforms into a self-crossing loop, with the self-crossing point marked by the magenta circle in Fig. 1(c). Next, we examine in Fig. 1(d) the complete band structure for the whole 2D Brillouin zone (BZ), with special attention paid to the bottom band. There, the self-crossing loop structure is found to form along both k_x and k_y dimensions. In particular, three looped subbands have grown from the bottom mother band (two of them at the edge of the shown BZ). Within the regime of each individual looped structure, Eq. (2) yields four Bloch states. Precisely at a self-crossing point of a looped subband, two of the four Bloch states are degenerate. The Chern number of the lowest band, which distinguishes between topologically trivial and nontrivial phases in noninteracting Dirac-Chern insulators, stays at the same value as its linear counterpart ($g = 0$) until $g = g_c$. For $g > g_c$, though the bottom mother band is still well separated from the upper band, its Chern number becomes ill defined due to the emergence of the self-crossing points. As such, it is necessary to study the bottom mother band individually from the perspective of a gapless topological phase.

Nonlinear Dirac cones. For the rest of our analysis, we set $J_x = J_y = 1$ and let $\mathcal{B} \equiv \mathcal{B}(0,0) = B(M+2)$. A simple calculation indicates that $g_c = 2\mathcal{B}$, beyond which Eq. (2) may host four stationary solutions for one given set of k_x and k_y. By considering Eq. (1) near one of the three self-crossing points seen in Fig. 1(d), e.g., at $k_x = k_y = 0$, we obtain the following energy solutions [51],

$$E_{\pm}(k_x,k_y) = \frac{g}{2} \pm \frac{1}{\sqrt{1-\frac{4\mathcal{B}^2}{g^2}}}\sqrt{k_x^2+k_y^2}, \tag{3}$$

where $+(-)$ stands for the upper (lower) energy branch around a self-crossing point. These energy solutions are isotropic in the k_x-k_y plane, linear with respect to the magnitude of the overall wave vector $k \equiv \sqrt{k_x^2+k_y^2}$. Analogous results linear in both k_x and k_y are found near other self-crossing points. We thus witness here the emergence of 2D self-crossing perfect Dirac cones for $g > g_c$, which we will refer to as nonlinear Dirac cones (NDCs).

We next rewrite Eq. (2) by making use of the above-obtained solutions and their corresponding eigenstates [51], arriving at two effective Hamiltonians for the positive and negative branches of the Dirac cone centered at $k_x = k_y = 0$,

$$h_{\text{eff},\pm} = k_x\sigma_x + k_y\sigma_y \mp \frac{2\mathcal{B}}{\sqrt{g^2-4\mathcal{B}^2}}\sqrt{k_x^2+k_y^2}\sigma_z. \tag{4}$$

That the two branches of the Dirac cone are described by different effective Hamiltonians is simply because $\mathcal{H}$ specified in Eq. (2) depends on the Bloch band state. As a consequence, the two Bloch band states associated with the positive and negative branches of the same Dirac cone are not orthogonal in general. Of particular importance and interest, $h_{\text{eff},\pm}$ differ from the familiar effective Hamiltonian of a conventional 2D Dirac cone [9,10], in that only $h_{\text{eff},\pm}$ found here has a σ_z (mass) term. The peculiar form of $h_{\text{eff},\pm}$ depicted in Eq. (4) has three implications detailed below.

First, NDCs are robust against generic local perturbations, similar to Weyl points in Weyl semimetals [12–15]. To understand this, note that a generic perturbation in two-level systems can be expressed in terms of the Pauli matrices σ_x, σ_y, and σ_z. As seen from $h_{\text{eff},\pm}$, perturbations proportional to σ_x or σ_y will only shift the location of the self-crossing point of an NDC in the k_x-k_y plane, e.g., perturbation of the form $h_x\sigma_x$ shifts the location of the self-crossing point from $(k_x,k_y) = (0,0)$ to $(k_x,k_y) = (-h_x,0)$. For a perturbation proportional to σ_z, i.e., a perturbative mass term (which opens a gap in conventional 2D Dirac cones), it can only renormalize the value of $\mathcal{B}$ [62]. This preserves NDCs again as long as g is not too close to g_c. These understandings are computationally confirmed in the Supplemental Material [51]. While a conventional 2D Dirac cone needs to be protected by certain symmetries, NDCs here are protected by interaction.

Second, the σ_z term of $h_{\text{eff},\pm}$ may be interpreted as a mass term. In that case, the mass m has to be momentum dependent, which is an exotic and counterintuitive result. Along this line, $h_{\text{eff},\pm}$ in Eq. (4) can then be rewritten as $h_{\text{eff},\pm} = ck_x\sigma_x + ck_y\sigma_y + m_{\pm}c^2\sigma_z$ in the same manner as a Dirac particle, with

$c = 1$, $m = \frac{2\mathcal{B}}{\sqrt{g^2-4\mathcal{B}^2}}k$. Further, the group velocity, i.e., the gradient of the energy band with respect to k near a Dirac point, is given by $\frac{g}{\sqrt{g^2-4\mathcal{B}^2}} > 1$. It depends on $\mathcal{B}$ and g, but stays always larger than $c = 1$, indicating a "superluminal" behavior. Namely, a quasiparticle described by an NDC may travel faster than the effective speed of light in the system. These features can be useful for the quantum simulation of the so-called tachyonic particle [63,64]. For example, it is of interest to look into the quantum Landau levels and Klein tunneling of such exotic quasiparticles.

Third, around the self-crossing point of an NDC, an interesting pseudospin texture arises. This can be appreciated more clearly by specifically writing down the Bloch band states in the NDC regime. Using $h_{\text{eff},\pm}$ in Eq. (4), one obtains the following Bloch band pseudospinors,

$$|\psi_\pm(k_x,k_y)\rangle = \begin{bmatrix} \cos\left(\frac{\theta}{2}\right) \\ \pm\sin\left(\frac{\theta}{2}\right)e^{i\phi(k_x,k_y)} \end{bmatrix}, \tag{5}$$

with

$$\tan[\phi(k_x,k_y)] = \frac{k_y}{k_x}, \quad \tan(\theta) = \frac{\mp\sqrt{g^2-4\mathcal{B}^2}}{2\mathcal{B}}. \tag{6}$$

Hence, within the NDC regime, the orientation of the Bloch state pseudospinor is in the (θ,ϕ) direction on the pseudospin Bloch sphere, with θ being independent of k_x and k_y. For g close to $g_c = 2\mathcal{B}$, the pseudospinor is aligned almost towards the north or south pole, and only for $g \gg g_c$, the pseudospinor is aligned almost towards the equator. In general situations, the pseudospinor may be aligned towards any direction. Consider then a parallel transport of the vector $|\psi_\pm(k_x,k_y)\rangle$ around the Dirac cone for one complete cycle ($\phi \to \phi + 2\pi$) (note that the Berry phase itself can be unrelated to any dynamical evolution). Both $|\psi_+(k_x,k_y)\rangle$ and $|\psi_-(k_x,k_y)\rangle$ are found to yield the same Berry phase γ, with

$$\begin{aligned}\gamma &= i\int \langle\psi_\pm(k_x,k_y)|\frac{d}{d\phi}|\psi_\pm(k_x,k_y)\rangle d\phi \\ &= \pi W_c[1-\cos(\theta)].\end{aligned} \tag{7}$$

Here, $W_c = 1$ is the winding number of the pseudospinor around a string pointing at the north pole. More generally, $W_c = \frac{1}{2\pi}\oint \frac{d\phi}{d\xi}d\xi$, with ξ being an arbitrary parameter of a cyclic path. In particular, the quantity πW_c, the topological part of the Berry phase [65], is by definition quantized in π. However, the overall Berry phase γ for one NDC is apparently not quantized. Rather, it changes continuously from $\gamma = 0$ to $\gamma = \pi$, as θ changes continuously from $\theta = 0$ (when $g \to g_c$ from above) to $\theta = \pi/2$ (when $g \gg g_c$). A computational example without making any approximation is shown in Fig. 2 (red line and black squares). There, the Berry phase is zero in the absence of an NDC. Once an NDC emerges within the area enclosed by a cyclic path in the momentum space, γ becomes continuously tunable with g. The computational results are in full agreement with our theory. The features of γ shown in Fig. 2 also indicate that γ can serve as an order parameter to signify the generation of one NDC by interaction.

Detection of NDCs and topological invariant. A recent study [48] demonstrated the detection of a conventional 2D Dirac cone by use of an interference setup, very similar

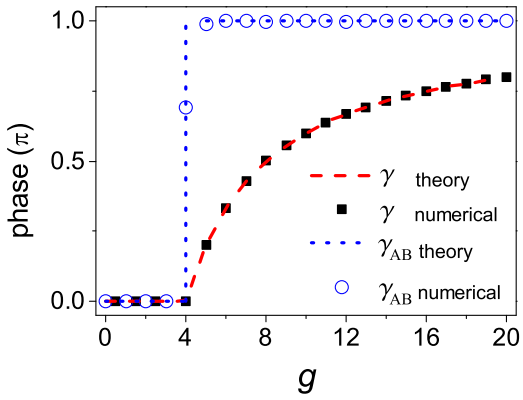

FIG. 2. The red dashed line and black squares depict the Berry phase γ associated with one nonlinear Dirac cone, obtained from theory and from direct numerical results based on the time-dependent GP equation. The blue line and circles are the adiabatic AB phase γ_{AB} associated with two interfering paths enclosing the same nonlinear Dirac cone, obtained theoretically or computationally. The system parameters chosen are $M = -1$, $B = 2$, and $J_x = J_y = 1$. The two interfering paths in the momentum space to generate the AB phase are chosen as two small semicircles going around the nonlinear Dirac cone, one clockwise and the other one counterclockwise. The system is forced to quasiadiabatically move along the two paths with $\frac{d\phi}{dt} = 10^{-3}$.

to an AB-effect experiment [49]. The two interfering paths enclosing a Dirac point are designed in the reciprocal (quasimomentum) space, with the beam splitting and recombination executed adiabatically by, for example, a certain spin-dependent (in our case, sublattice-dependent) force [48]. Consider then this interference approach: Two interfering paths share the same starting point [see Fig. 1(e)] and both go around a Dirac point in a symmetric manner, with one clockwise and the other one counterclockwise. In the NDC regime with all other system parameters fixed, the θ parameter given in Eq. (6) is a constant along each path. Hence only the ϕ parameter [also defined in Eq. (6)] suffices to parametrize the two paths. After the system has been forced to adiabatically travel along the two respective paths, we look into their quantum phase difference, called the adiabatic AB phase here. Explicit implementations of how the initial Bloch state is split and recombined, as well as how quasimomenta k_x and k_y are adiabatically varied, are not needed in our computational and theoretical studies below.

It is tempting to associate the adiabatic AB phase with the Berry phase γ in Eq. (7). However, computational results clearly indicate that they are different. As depicted by the blue circles in Fig. 2, the adiabatic AB phase is zero in the absence of NDCs ($g < g_c$). However, as long as $g > g_c$, the adiabatic AB phase changes discontinuously to π. That is, contrary to the continuous behavior of γ shown above, the adiabatic AB phase is actually quantized in π. For the computational results shown in Fig. 2, the two paths enclosing an NDC are chosen to be two small semicircles. We have considered other path geometries and the same results are obtained. The experimentally measurable AB phase obtained here is thus smoking-gun evidence of the formation of an NDC.

Note that the detection of the AB phase necessarily involves a process of dynamical evolution. Indeed, the system is designed to adiabatically evolve along two different paths. During this process, though ϕ changes very slowly at a small rate ϵ, the system cannot be precisely on its instantaneous Bloch states $|\psi(k_x,k_y)\rangle$. Instead, to the first order of ϵ, the system's actual time-evolving state $|\Psi(t)\rangle$ is given by

$$|\Psi(t)\rangle = |\psi(k_x,k_y)\rangle + \epsilon|\delta\psi(t)\rangle. \tag{8}$$

This adiabatic perturbation to the first order of ϵ has a nontrivial impact on the nonlinear Hamiltonian $\mathcal{H}[k_x,k_y,\Psi(t)]$ governing the dynamics [66,67], resulting in

$$\mathcal{H}[k_x,k_y,\Psi(t)] = \mathcal{H}[k_x,k_y,\psi(k_x,k_y)] + h_{\rm NA} + O(\epsilon^2), \tag{9}$$

where $h_{\rm NA}$ stands for the first-order nonadiabatic contribution to the system's instantaneous effective Hamiltonian $\mathcal{H}[k_x,k_y,\psi(k_x,k_y)]$. Using the first-order perturbation theory and Eq. (5), we find that $h_{\rm NA}$ is rather simple [51],

$$h_{\rm NA} = \frac{1}{2}\sigma_z \frac{d\phi(k_x,k_y)}{dt}. \tag{10}$$

Note that the first-order energy correction due to $h_{\rm NA}$, i.e., $\mathcal{E}_{\rm NA} = \langle\psi(k_x,k_y)|h_{\rm NA}|\psi(k_x,k_y)\rangle$, is simply given by $\frac{1}{2}\cos(\theta)\frac{d\phi(k_x,k_y)}{dt}$. As a useful observation, the two paths now yield different $\mathcal{E}_{\rm NA}$ as energy corrections because their $\frac{d\phi(k_x,k_y)}{dt}$ has different signs.

Consider then the dynamical phase along each path, which is obtained as an integral of $E_{\pm}(k_x,k_y) + \mathcal{E}_{\rm NA}$, i.e., the expectation value of $\mathcal{H}[k_x,k_y,\Psi(t)] = \mathcal{H}[k_x,k_y,\psi(k_x,k_y)] + h_{\rm NA}$, over a time scale of the order ϵ^{-1}. Clearly then, though $\mathcal{E}_{\rm NA}$ is of the order of ϵ, with its impact accumulated over time of the order ϵ^{-1}, it can still make a contribution of the order of ϵ^0 to the dynamical phase. Further, we note that the dynamical phase contributed by $E_{\pm}(k_x,k_y)$ is identical for two symmetric interfering paths on the same branch of an NDC. Thus, only $\mathcal{E}_{\rm NA}$ introduces an ϵ-*independent* dynamical phase difference $\Delta\gamma_{\rm dyn}$ between the two adiabatic paths, with

$$\begin{aligned}\Delta\gamma_{\rm dyn} &= \frac{1}{2}\cos(\theta)\left[\int_0^{\pi} d\phi - \int_0^{-\pi} d\phi\right] \\ &= \pi\cos(\theta).\end{aligned} \tag{11}$$

The adiabatic AB phase produced by the two interfering paths is then given by $\Delta\gamma_{\rm dyn}$ obtained above *plus* their geometric phase difference. Recognizing that their geometric phase difference is simply the previously found Berry phase γ (dropping a negligible correction of the order of ϵ), we obtain the adiabatic AB phase as the following,

$$\gamma_{\rm AB} = \gamma + \Delta\gamma_{\rm dyn} = \pi W_c. \tag{12}$$

That is, $\Delta\gamma_{\rm dyn}$ precisely cancels the nontopological part of the Berry phase γ, yielding an adiabatic AB phase quantized in π. This fully explains the computational results presented in Fig. 2 (see the blue dashed line and circles). Our theory here also identifies the winding number W_c as an observable topological invariant of NDCs. In our numerically exact calculations, we also find that if the rate of change in ϕ is increased by ten times from what is considered in Fig. 2, the quantization of the AB phase is only slightly degraded due to nonadiabatic effects beyond the first order of ϵ.

Discussion and conclusions. It is also of interest to discuss the role of the system parameter M. In the noninteracting Dirac-Chern insulator model, cases with $|M| > 2$ ($|M| < 2$) represent a topologically trivial (nontrivial) phase [50], with a topological phase transition at $M = 2$. The same behavior is observed in the interacting case with $g < g_c$. Interestingly, with the emergence of NDCs [$g > g_c = 2B(M+2)$], regardless of the value of M, their topological invariant W_c stays to be unity and the adiabatic AB phase remains quantized in π. In particular, for $g > 8B$, phases with $|M| > 2$ and those with $|M| < 2$ all have the same topological invariant and hence they can be categorized into the same (gapless) topological phase. This clearly shows the possibility of two topologically distinct phases to become topologically equivalent as an outcome of interaction [21], thus revealing the interplay of topology and nonlinearity. About possible experimental studies, one potential issue is the dynamical stability [56] of our nonlinear two-band model. We have checked that near a looped subband, the lower main band is dynamically stable in the presence of perturbations that respect the translational symmetry of the system (see Supplemental Material [51]).

In conclusion, we have discovered a nonlinearity-induced quantum phase transition from a known topological insulating phase to a different gapless topological phase featured by NDCs. The NDCs are robust against local perturbations without symmetry restrictions. In addition, they have peculiar pseudospin textures, remarkable band structures, and nonquantized Berry phases. By showing that an adiabatic AB phase is still quantized in π, we have identified a winding number as a directly measurable topological invariant of such nonlinear Dirac cones.

Acknowledgments. J.G. is supported by the Singapore NRF Grant No. NRF-NRFI2017-04 (WBS No. R-144-000-378-281) and by the Singapore Ministry of Education Academic Research Fund Tier I (WBS No. R-144-000-353-112). W.Z. is supported by the National Natural Science Foundation of China (Grant No. 11447016).

[1] D. J. Thouless, M. Kohmoto, M. P. Nightingale, and M. den Nijs, Quantized Hall Conductance in a Two-Dimensional Periodic Potential, Phys. Rev. Lett. **49**, 405 (1982).

[2] D. J. Thouless, Quantization of particle transport, Phys. Rev. B **27**, 6083 (1983).

[3] D. Hsieh, D. Qian, L. Wray, Y. Xia, Y. S. Hor, R. J. Cava, and M. Z. Hasan, A topological Dirac insulator in a quantum spin Hall phase, Nature (London) **452**, 970 (2008).

[4] H. Zhang, C.-X. Liu, X.-L. Qi, X. Dai, Z. Fang, and S.-C. Zhang, Topological insulators in Bi_2Se_3, Bi_2Te_3, and Sb_2Te_3

with a single Dirac cone on the surface, Nat. Phys. **5**, 438 (2009).

[5] Y. Xia, D. Qian, D. Hsieh, L. Wray, A. Pal, H. Lin, A. Bansil, D. Grauer, and Y. S. Hor, Observation of a large-gap topological-insulator class with a single Dirac cone on the surface, Nat. Phys. **5**, 398 (2009).

[6] K. S. Novoselov, A. K. Geim, S. V. Morozov, D. Jiang, M. I. Katsnelson, I. V. Grigorieva, S. V. Dubonos, and A. A. Firsov, Two-dimensional gas of massless Dirac fermions in graphene, Nature (London) **438**, 197 (2005).

[7] E. F. Foa Torres, S. Roche, and J.-C. Charlier, *Introduction to Graphene-Based Nanomaterials* (Cambridge University Press, Cambridge, UK, 2014).

[8] Y. Zhang, Y. Tan, H. L. Stormer, and P. Kim, Experimental observation of the quantum Hall effect and Berry's phase in graphene, Nature (London) **438**, 201 (2005).

[9] Z. Wang, Y. Sun, X.-Q. C, C. Franchini, G. Xu, H. Weng, X. Dai, and Z. Fang, Dirac semimetal and topological phase transitions in A_3Bi (A = Na, K, Rb), Phys. Rev. B **85**, 195320 (2012).

[10] S. M. Young, S. Zaheer, J. C. Y. Teo, C. L. Kane, E. J. Mele, and A. M. Rappe, Dirac Semimetal in Three Dimensions, Phys. Rev. Lett. **108**, 140405 (2012).

[11] S. M. Young and C. L. Kane, Dirac Semimetals in Two Dimensions, Phys. Rev. Lett. **115**, 126803 (2015).

[12] X. Wan, A. M. Turner, A. Vishwanath, and S. Y. Savrasov, Topological semimetal and Fermi-arc surface states in the electronic structure of pyrochlore iridates, Phys. Rev. B **83**, 205101 (2011).

[13] A. A. Burkov, M. D. Hook, and L. Balents, Topological nodal semimetals, Phys. Rev. B **84**, 235126 (2011).

[14] S.-Y. Xu, I. Belopolski, N. Alidoust, M. Neupane, G. Bian, C. Zhang, R. Sankar, G. Chang, Z. Yuan, C.-C. Lee, S.-M. Huang, H. Zheng, J. Ma, D. S. Sanchez, B. Wang, A. Bansil, F. Chou, P. P. Shibayev, H. Lin, S. Jia, and M. Z. Hasan, Discovery of a Weyl fermion semimetal and topological Fermi arcs, Science **349**, 613 (2015).

[15] H. Weng, C. Fang, Z. Fang, B. A. Bernevig, and X. Dai, Weyl Semimetal Phase in Noncentrosymmetric Transition-Metal Monophosphides, Phys. Rev. X **5**, 011029 (2015).

[16] T. T. Heikkilä and G. E. Volovik, Dimensional crossover in topological matter: Evolution of the multiple Dirac point in the layered system to the flat band on the surface, JETP Lett. **93**, 59 (2011).

[17] C. Fang, Y. Chen, H.-Y. Kee, and L. Fu, Topological nodal line semimetals with and without spin-orbital coupling, Phys. Rev. B **92**, 081201(R) (2015).

[18] G. Bian, T.-R. Chang, R. Sankar, S.-Y. Xu, H. Zheng, T. Neupert, C.-K. Chiu, S.-M. Huang, G. Chang, I. Belopolski, D. S. Sanchez, M. Neupane, N. Alidoust, C. Liu, B. Wang, C.-C. Lee, H.-T. Jeng, C. Zhang, Z. Yuan, S. Jia, A. Bansil, F. Chou, H. Lin, and M. Z. Hasan, Topological nodal-line fermions in spin-orbit metal $PbTaSe_2$, Nat. Commun. **7**, 10556 (2016).

[19] G. Bian, T.-R. Chang, H. Zheng, S. Velury, S.-Y. Xu, T. Neupert, C.-K. Chiu, S.-M. Huang, D. S. Sanchez, I. Belopolski, N. Alidoust, P.-J. Chen, G. Chang, A. Bansil, H.-T. Jeng, H. Lin, and M. Z. Hasan, Drumhead surface states and topological nodal-line fermions in $TlTaSe_2$, Phys. Rev. B **93**, 121113(R) (2016).

[20] C. Fang, H. Weng, X. Dai, and Z. Fang, Topological nodal line semimetals, Chin. Phys. B **25**, 117106 (2016).

[21] L. Fidkowski and A. Kitaev, Effects of interactions on the topological classification of free fermion systems, Phys. Rev. B **81**, 134509 (2010).

[22] L. Fidkowski and A. Kitaev, Topological phases of fermions in one dimension, Phys. Rev. B **83**, 075103 (2011).

[23] C. N. Varney, K. Sun, M. Rigol, and V. Galitski, Topological phase transitions for interacting finite systems, Phys. Rev. B **84**, 241105(R) (2011).

[24] C. Wang, A. C. Potter, and T. Senthil, Classification of interacting electronic topological insulators in three dimensions, Science **343**, 629 (2014).

[25] H. Isobe and L. Fu, Theory of interacting topological crystalline insulators, Phys. Rev. B **92**, 081304 (2015).

[26] R.-X. Zhang, C. Xu, and C.-X. Liu, Interacting topological phases in thin films of topological mirror Kondo insulators, Phys. Rev. B **94**, 235128 (2016).

[27] X.-Y. Song and A. P. Schnyder, Interaction effects on the classification of crystalline topological insulators and superconductors, Phys. Rev. B **95**, 195108 (2017).

[28] A. P. Schnyder, S. Ryu, A. Furusaki, and A. W. W. Ludwig, Classification of topological insulators and superconductors in three spatial dimensions, Phys. Rev. B **78**, 195125 (2008).

[29] A. Kitaev, Periodic table for topological insulators and superconductors, in *Advances in Theoretical Physics: Landau Memorial Conference*, edited by V. Lebedev and M. Feigel'man, AIP Conf. Proc. Vol. 1134 (AIP, Melville, NY, 2009), p. 22.

[30] *Topological Aspects of Condensed Matter Physics*, edited by C. Chamon, M. O. Goerbig, R. Moessner, and L. F. Cugliandolo (Oxford University Press, Oxford, UK, 2017).

[31] C.-E. Bardyn, T. Karzig, G. Refael, and T. C. H. Liew, Chiral Bogoliubov excitations in nonlinear bosonic systems, Phys. Rev. B **93**, 020502(R) (2016).

[32] D. R. Gulevich, D. Yudin, D. V. Skryabin, I. V. Iorsh, and I. A. Shelykh, Exploring nonlinear topological states of matter with exciton-polaritons: Edge solitons in kagome lattice, Sci. Rep. **7**, 1780 (2017).

[33] D. Leykam and Y. D. Chong, Edge Solitons in Nonlinear-Photonic Topological Insulators, Phys. Rev. Lett. **117**, 143901 (2016).

[34] O. Bleu, D. D. Solnyshkov, and G. Malpuech, Interacting quantum fluid in a polariton Chern insulator, Phys. Rev. B **93**, 085438 (2016).

[35] O. Bleu, D. D. Solnyshkov, and G. Malpuech, Photonic versus electronic quantum anomalous Hall effect, Phys. Rev. B **95**, 115415 (2017).

[36] C. Liu, Z. Wang, C. Yin, Y. Wu, T. Xu, L. Wen, and S. Chen, The nontrivial states in one-dimensional nonlinear bichromatic superlattices, Physica E (Amsterdam) **90**, 183 (2017).

[37] E. P. Gross, Structure of a quantized vortex in boson systems, Nuovo Cimento **20**, 454 (1961).

[38] L. P. Pitaevskii, Vortex lines in an imperfect Bose gas, JETP **13**, 451 (1961).

[39] S. Burger, K. Bongs, S. Dettmer, W. Ertmer, K. Sengstock, A. Sanpera, G. V. Shlyapnikov, and M. Lewenstein, Dark Solitons in Bose-Einstein Condensates, Phys. Rev. Lett. **83**, 5198 (1999).

[40] J. Denschlag, J. E. Simsarian, D. L. Feder, C. W. Clark, L. A. Collins, J. Cubizolles, L. Deng, E. W. Hagley, K. Helmerson, W. P. Reinhardt, S. L. Rolston, B. I. Schneider, and W. D. Phillips, Generating solitons by phase engineering of a bose-einstein condensate, Science **287**, 97 (2000).

[41] K. E. Strecker, G. B. Partridge, A. G. Truscott, and R. G. Hulet, Formation and propagation of matter-wave soliton trains, Nature (London) **417**, 150 (2002).

[42] Y. Lumer, Y. Plotnik, M. C. Rechtsman, and M. Segev, Self-Localized States in Photonic Topological Insulators, Phys. Rev. Lett. **111**, 243905 (2013).

[43] Y. Plotnik, M. C. Rechtsman, D. Song, M. Heinrich, J. M. Zeuner, S. Nolte, Y. Lumer, N. Malkova, J. Xu, A. Szameit, Z. Chen, and M. Segev, Observation of unconventional edge states in "photonic graphene," Nat. Mater. **13**, 57 (2014).

[44] G. Jotzu, M. Messer, R. Desbuquois, M. Lebrat, T. Uehlinger, D. Greif, and T. Esslinger, Experimental realization of the topological Haldane model with ultracold fermions, Nature (London) **515**, 237 (2014).

[45] N. Goldman, J. C. Budich, and P. Zoller, Topological quantum matter with ultracold gases in optical lattices, Nat. Phys. **12**, 639 (2016).

[46] L. Lu, J. D. Joannopoulos, and M. Soljačič, Topological photonics, Nat. Photonics **8**, 821 (2014).

[47] B. Wu and Q. Niu, Nonlinear Landau-Zener tunneling, Phys. Rev. A **61**, 023402 (2000).

[48] L. Duca, T. Li, M. Reitter, I. Bloch, M. Schleier-Smith, and U. Schneider, An Aharonov-Bohm interferometer for determining Bloch band topology, Science **347**, 288 (2015).

[49] Y. Aharonov and D. Bohm, Significance of electromagnetic potentials in the quantum theory, Phys. Rev. **115**, 485 (1959).

[50] X.-L. Qi, Y.-S. Wu, and S.-C. Zhang, Topological quantization of the spin Hall effect in two dimensional paramagnetic semiconductors, Phys. Rev. B **74**, 085308 (2006).

[51] See Supplemental Material at http://link.aps.org/supplemental/10.1103/PhysRevB.96.121406 for derivations of $\mathcal{H}[k_x,k_y,\psi(k_x,k_y)]$, $E_{\pm}(k_x,k_y)$, $h_{\mathrm{eff},\pm}$, h_{NA}, and for computational examples confirming the robustness of NDCs, as well as computational details about Fig. 2.

[52] B. A. Bernevig, T. L. Hughes, and S.-C. Zhang, Quantum spin Hall effect and topological phase transition in HgTe quantum wells, Science **314**, 1757 (2006).

[53] M. König, S. Wiedmann, C. Brüne, A. Roth, H. Buhmann, L. W. Molenkamp, X.-L. Qi, and S.-C. Zhang, Quantum spin Hall insulator state in HgTe quantum wells, Science **318**, 766 (2007).

[54] E. J. Mueller, Superfluidity and mean-field energy loops: Hysteretic behavior in Bose-Einstein condensates, Phys. Rev. A **66**, 063603 (2002).

[55] M. Machholm, C. J. Pethick, and H. Smith, Band structure, elementary excitations, and stability of a Bose-Einstein condensate in a periodic potential, Phys. Rev. A **67**, 053613 (2003).

[56] B. Wu and Q. Niu, Superfluidity of Bose-Einstein condensate in an optical lattice: Landau-Zener tunneling and dynamical instability, New J. Phys. **5**, 104 (2003).

[57] G. F. Wang, D. F. Ye, L. B. Fu, X. Z. Chen, and J. Liu, Landau-Zener tunneling in a nonlinear three-level system, Phys. Rev. A **74**, 033414 (2006).

[58] G. Watanabe, B. P. Venkatesh, and R. Dasgupta, Nonlinear phenomena of ultracold atomic gases in optical lattices: Emergence of novel features in extended states, Entropy **18**, 118 (2016).

[59] S. B. Koller, E. A. Goldschmidt, R. C. Brown, R. Wylie, R. M. Wilson, and J. V. Porto, Nonlinear looped band structure of Bose-Einstein condensates in an optical lattice, Phys. Rev. A **94**, 063634 (2016).

[60] Q. Zhang, P. Hänggi, and J. B. Gong, Two-mode Bose-Einstein condensate in a high-frequency driving field that directly couples the two modes, Phys. Rev. A **77**, 053607 (2008).

[61] S. Eckel, J. G. Lee, F. Jendrzejewski, N. Murray, C. W. Clark, C. J. Lobb, W. D. Phillips, M. Edwards, and G. K. Campbell, Hysteresis in a quantized superfluid atomtronic circuit, Nature (London) **506**, 200 (2014).

[62] Note that a perturbation $h_z\sigma_z$ will not simply appear as an additional term in the effective Hamiltonian. Instead, we need to return to Eq. (1) and retrace our derivation leading to Eq. (4). By inspection, such a perturbative mass term will simply combine with $\mathcal{B}$ to become $\mathcal{B}' = \mathcal{B} + h_z$. Consequently, Eq. (4) will retain its form, with $\mathcal{B}$ being replaced by $\mathcal{B}'$.

[63] G. Feinberg, Possibility of Faster-Than-Light Particles, Phys. Rev. **159**, 1089 (1967).

[64] V. M. Apalkov and T. Chakraborty, Superluminal tachyon-like excitations of Dirac fermions in a topological insulator junction, Europhys. Lett. **100**, 17002 (2012).

[65] J. N. Fuchsa, F. Piéchon, M. O. Goerbig, and G. Montambaux, Topological Berry phase and semiclassical quantization of cyclotron orbits for two-dimensional electrons in coupled band models, Eur. Phys. J. B **77**, 351 (2010).

[66] J. Liu and L. B. Fu, Berry phase in nonlinear systems, Phys. Rev. A **81**, 052112 (2010).

[67] Q. Zhang, J. B. Gong, and C. H. Oh, Dynamical fluctuations in classical adiabatic processes: General description and their implications, Ann. Phys. **327**, 1202 (2012).